Comparative Approaches for Quantification of Product Yield in a Model Recombinant Green Fluorescent Protein Expressed in *E. coli*

By Gabrielle Rusch[1,2], Junhyeong Wang[3], Keith Breau[4], Katie Kilgour[5], Gary Gilleskie[6], Jeff Keele[6], Kurt Selle[6], Scott T. Magness[1], Stefano Menegatti[5*], and Michael Daniele[1,2*]

[1] Joint Department of Biomedical Engineering
North Carolina State University and University of North Carolina, Chapel Hill
911 Oval Dr., Raleigh, NC 27695 (USA)

[2] Comparative Medicine Institute
North Carolina State University
1060 William Moore Dr., Raleigh, NC 27606 (USA)

[3] Department of Electrical & Computer Engineering
North Carolina State University
890 Oval Dr., Raleigh NC, 27695 (USA)

[4] Department of Cell Biology and Physiology
University of North Carolina, Chapel Hill
111 Mason Farm Road, Chapel Hill, NC 27599 (USA)

[5] Department of Chemical Engineering
North Carolina State University
911 Partners Way, Raleigh, NC 27695 (USA)

[6] Golden LEAF Biomanufacturing Training and Education Center (BTEC)
NC State University, Raleigh, NC 27695 (USA)

[*] Correspondence: mdaniel6@ncsu.edu; smenega@ncsu.edu

ABSTRACT

Process Analytical Technologies (PAT) used to monitor and control manufacturing processes are crucial for efficient and automated bioprocessing, which is in congruence with lights-off-manufacturing and Industry 4.0 initiatives. As biomanufacturing seeks to realize more high-throughput and automated operation, an increasing need for multimodal analysis of process metrics becomes essential. Herein, we detail a series of methods for analyzing product yield from a bioreactor and how to conduct cross-method comparisons. We employ a model system of *Escherichia coli* (*E. coli*) expression of green fluorescent protein (GFP), which is a simple, cost effective model for students and educators to replicate at different scales. GFP is an ideal analytical marker as it is easy to visualize due to its fluorescence which indicates cellular protein expression, cell localization and physiological changes of the cell population. In this study, samples from a 300 L bioreactor with GFP-expressing *E. coli* are analyzed to improve product yield and bioprocessing efficiency. Utilizing a fed-batch process for enhanced cell density and product titer, this bioreactor runs on a 24-hour schedule from inoculation to GFP induction and final harvest. To reliably quantify relative GFP expression and *E. coli* proliferation, we provide simple protocols and example results for comparing three different analytical methods: (1) in-line bioreactor measurements, (2) plate reader assays, and (3) microscopy. The GFP and cell density results follow similar trends based on the various inline and offline analytical methods and show a peak of GFP expression and cell density between 12.5 and 18 hours post inoculation.

KEYWORDS:

Bioreactor, GFP, Process Analytical Technologies, Fluorescence Microscopy, Image Analysis

1. INTRODUCTION

Optimized bioprocessing is essential for large-scale production of biotechnological products ranging from chemicals to pharmaceuticals and advanced cell therapies like CAR-T cells and stem cells. [1], [2] To ensure streamlined manufacturing and high yield, variables such as temperature, chemical composition, pressure and pH are tightly regulated and monitored throughout bioprocesses. [3] Process analytical technologies (PAT), used to measure and control critical manufacturing attributes, provide comprehensive insight necessary for manufacturing optimization and quality assurance. [4]

The future of "off-the-shelf" cellular therapies and drug solutions holds great promise with the adoption of continuous manufacturing techniques. [5] This manufacturing approach, integrated with advanced PAT, ensures the consistent production of high-quality therapeutics at a reduced cost, effectively meeting the escalating market demand. [5, 6] Employing and advancing PAT will become increasingly important as biomanufacturing transitions from traditional batch processing to large scale continuous manufacturing platforms. [7], [8]

PAT includes inline, at-line, and offline analytical approaches crucial for ensuring the efficiency, quality, and safety of biotechnological production. [9] Inline analysis involves the real-time monitoring of critical parameters during the ongoing process within the bioprocessing system itself. This is achieved through the integration of probes and sensors that provide instantaneous and continuous data collection of variables such as pH, dissolved oxygen, and temperature. [10] At-line analysis involves sampling from the process stream for analysis. While not continuous, at-line methods allow for more specialized measurements which are not fully integrated into the biomanufacturing pipeline. Offline analysis entails the collection of samples from the bioprocess for analysis in a laboratory setting, often using instrumentation or techniques not suitable for real-time monitoring. Although not as immediate as inline or at-line methods, this method provides valuable information for process optimization, quality assurance, and regulatory compliance. [11] Together, these complementary analytical approaches form a comprehensive toolkit for monitoring and optimizing bioprocesses, ensuring the consistent production of high-quality biotechnological products.

The utilization of green fluorescent protein (GFP) as a reporter molecule has become a cornerstone in bioprocess monitoring, offering researchers a versatile tool for real-time visualization and quantification of protein expression dynamics within microbial hosts. [12], [13] Typically induced through isopropyl β-D-1-thiogalactopyranoside (IPTG) or temperature changes, GFP expression cultivates alongside rapid cell proliferation. By genetically fusing GFP with the protein of interest or co-expressing it alongside, researchers can monitor temporal and spatial aspects of protein production throughout the bioprocess continuum. Furthermore, GFP serves as a quantitative indicator of protein yield, enabling rapid assessment of culture conditions and optimization of bioprocess parameters. Through high-throughput screening methodologies, GFP facilitates the identification of high-producing microbial clones, expediting strain development endeavors. Thus, this review underscores GFP's pivotal role in advancing bioprocess monitoring techniques, offering insights into its applications, challenges, and prospects in biomanufacturing. [14]

By utilizing induced Green Fluorescent Protein (GFP) expression of *Escherichia coli (E. coli)* cultivated in a 300 L bioreactor resembling conditions in large-scale industrial bioprocessing, we explored and compared various analytical techniques which are commonly used in biomanufacturing practices. GFP expression provides insights into cellular activity such as cell proliferation and protein expression which can be used to optimize bioprocess parameters. [15] Induction of GFP expression in *E. coli* relies on the introduction of isopropyl β-D-1-thiogalactopyranoside (IPTG) or temperature changes, which accelerates fluorescent marker expression and proliferation simultaneously. [16], [17], [18] This paper offers several methods for inline bioreactor analytics as well as offline analysis of cell proliferation and GFP expression during this bioprocess with respect to time as seen in Figure 1.

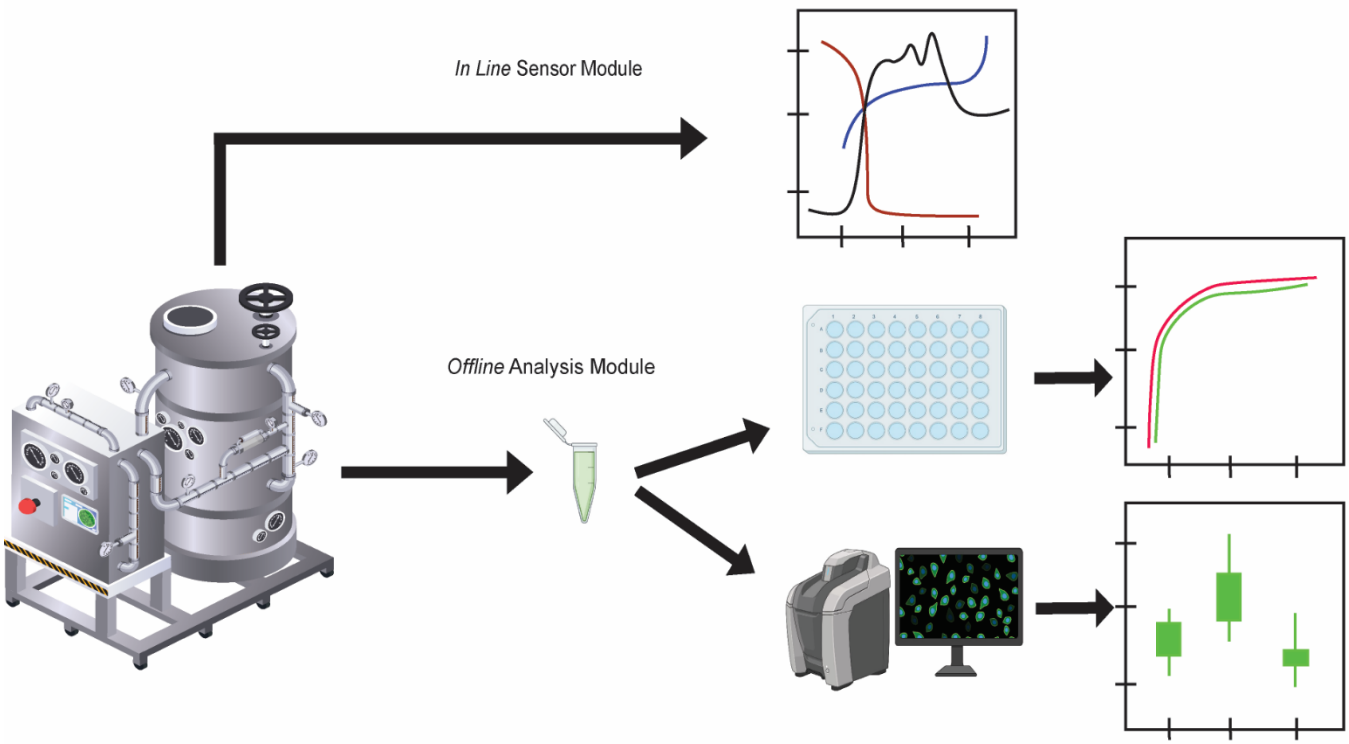

Figure 1. Overview of inline and offline analysis for this bioprocess. *Data was collected from several in line sensor modules to be compared against offline analytics including absorbance measurements from a plate reader and confocal image analysis to better understand the bioreactor performance.*

2. MATERIALS & METHODS

Bioreactor Preparation, Inoculation, GFP Induction and Harvest

The 300 L bioreactor used in this bioprocess employs a fed-batch approach to increase cell density and product titer. This bioreactor hosted GFP expressing *E.coli* suspended in culture broth for a 24-hour period. The setup encompassed bioreactor cleaning, raw material preparation, autoclaving, bioreactor assembly, pressure testing, introduction of *E.coli* and a series of batch processing steps prior to the induction of GFP expression through addition of isopropyl β-D-1-thiogalactopyranoside (IPTG) to the bioreactor solution. The protocol concluded with the harvest of the culture and review of both inline and offline analytics. After bioreactor set-up, the bioreactor was inoculated (*E.coli* introduced to the culture) and several hours later GFP was induced by the addition of IPTG. The bioreactor ran for 24 hours until the final batch was harvested. Two separate bioreactor runs were analyzed in this paper. Several metrics were measured inline during the bioreactor run including Optical Density (OD), glucose levels, pH, percentage of dissolved oxygen (DO%), temperature, and weight of the system. The solution was agitated throughout the 24 hour time and the rotations per minute (rpm) of mixing as well as standard liters per minute (slpm) of air sparging were recorded.

Sample Collection

Two separate bioreactor runs were analyzed. For both runs, two 1 mL samples were collected at designated time intervals during the process and placed in a -80ºC freezer prior to analysis. At hour 0, the bioreactor was inoculated and *E.coli* was added to the bioreactor. At hour 6, GFP expression was induced through addition of IPTG and final harvest occurred at hour 24. Samples were collected every hour post inoculation (hour 0), pre GFP induction (hour 6). Post induction (hour 6), samples were collected every 30 minutes until final harvest (hour 24). For cell density and GFP expression analysis, five time points S1 (Immediately after inoculation), S2 (7.5 hours post inoculation, S3 (12.5 hours post inoculation), S4 (18 hours post inoculation) and S5 (24 hours post inoculation) were used. The timeline of sample collection and bioreactor events are shown in Figure 2.

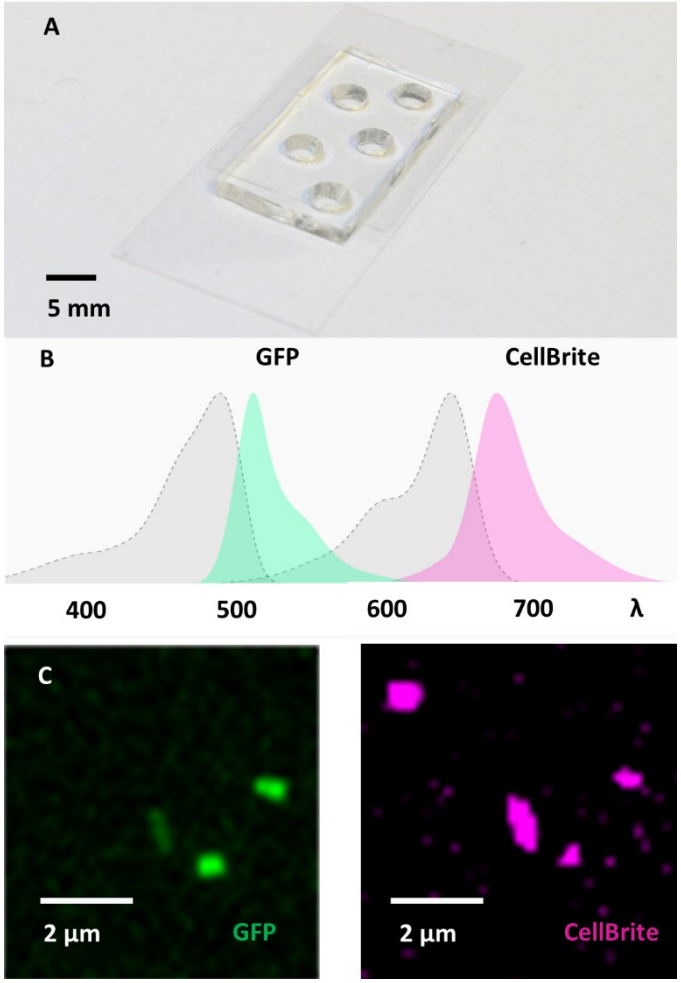

Figure 2. Microdevice used for confocal imaging of E.coli samples *a) The device was manufactured using PDMS bonded to a micro glass slide. Five hole punches were included for each of the five samples that were analyzed. b) The two excitation wavelengths for GFP and CellBrite are 495 and 640 nm, respectively. c) The GFP image compared with the CellBrite stained image.*

Plate Reader Assays

Absorbance and fluorescence intensity were measured on a Cytiva XYB98 plate reader. Absorbance (OD) was measured at λ = 600 nm and fluorescence intensity at λ_{ex} = 395 nm and λ_{em} = 508 nm. The OD values relate to cell density while fluorescence intensity relates to GFP expression. Samples were thawed and 100 uL was dispensed into 96 well plates. Each sample underwent thawing and 100 µL of each sample was dispensed into a black 96-well plate with a clear bottom for analysis. Technical triplicates were prepared and analyzed for each sample from both bioreactor runs. Following sample preparation and initial absorbance and fluorescence measurements were recorded, the plates were subjected to centrifugation at 4000xg for 3 minutes. Post-centrifugation, the supernatant was aspirated and plated alongside the pellet. Absorbance and fluorescence measurements were then recorded.

Confocal Microscopy and Image Analysis with Image J

Cells were also analyzed using a secondary offline analytical technique, confocal microscopy and image analysis. Prior to imaging, samples were thawed and 500 µL of each sample was removed, stained with CellBrite 640, fixed using 4% paraformaldehyde (PFA), and washed with PBS following standard protocols. After fixing, staining, and washing, each sample was resuspended in 5 mL of phosphate-buffered saline (PBS) and further diluted 1:200 for optimal imaging density. However, sample S1 from hour 0 contained a low cell count for both runs, necessitating a 1:20 dilution instead of the standard 1:200 dilution. This difference in dilution was accounted for in the image analysis. For ease of imaging multiple samples, microdevices were fabricated using polydimethylsiloxane (PDMS) bound to thin glass slides, including five wells made from hole punches for each

sample. These wells were then filled with 25 μL of each diluted sample. We used a laser scanning confocal microscope (LSCM) and all images were taken using a water immersion 63 x objective. GFP images were collected at λ_{ex} = 488 nm; λ_{em} = 507 nm set at 50.3% gain and 1.5% intensity, while the CellBrite 640 nm membrane stain images were collected at λ_{ex} = 642 nm; λ_{em} = 662 nm adjusted between 16-25% gain and 1.5% intensity for image acquisition. The membrane stain facilitated the identification of individual *E. coli* cells regardless of GFP expression to construct an imaging mask. When collecting CellBrite stain images, the gain and intensity were modified slightly from sample to sample, however the GFP images were collected at the same gain and intensity to allow for appropriate comparison of relative fluorescence per *E.coli*. The zoom was set to 1.0 and the pinhole was set to 1.00 AU for consistency in image capture. Images were collected until hundreds of individual *E.coli* were counted in each sample group. Each image was analyzed to determine cell count and fluorescence per cell using Image J as shown in Figure 2.

Image Analysis

Post image acquisition, all images were analyzed using Image J. The python script used details the general guideline to follow for repeatable measurements for both fluorescence intensity per *E.coli* and cell count per image. The code allowed for a repeatable image analysis for accurate comparison of relative GFP expression per *E.coli* and total cell count.

3. RESULTS & DISCUSSION

Bioreactor Metric Analysis

During the bioreactor run, several inline parameters were measured throughout the 24-hour process, which can be seen in Figure 3. The measured variables included optical density (OD) which increased with *E.coli* proliferation and glucose which decreased as *E. coli* proliferated and consumed. The weight of the entire sample was measured to ensure it was unchanged and maintained within a specific range (275 kg+/- 10 kg), although some variability in this measurement existed due to removal of samples throughout the process and standard measuring error. Agitation began in response to changes in DO and the rpm was recorded. The dissolved oxygen content (DO), which indicates how much oxygen has been consumed by the *E. coli* was recorded along with the air sparging standard liter per minute (slpm) which is used to promote mixing and aeration in the culture medium. The pH was maintained between 6-7, temperature was also tightly regulated between 29.8 and 30.1 C, and finally pressure which is maintained between 4.95 and 5.05 psi. Figure 3 shows the change in these metrics over time for run 2.

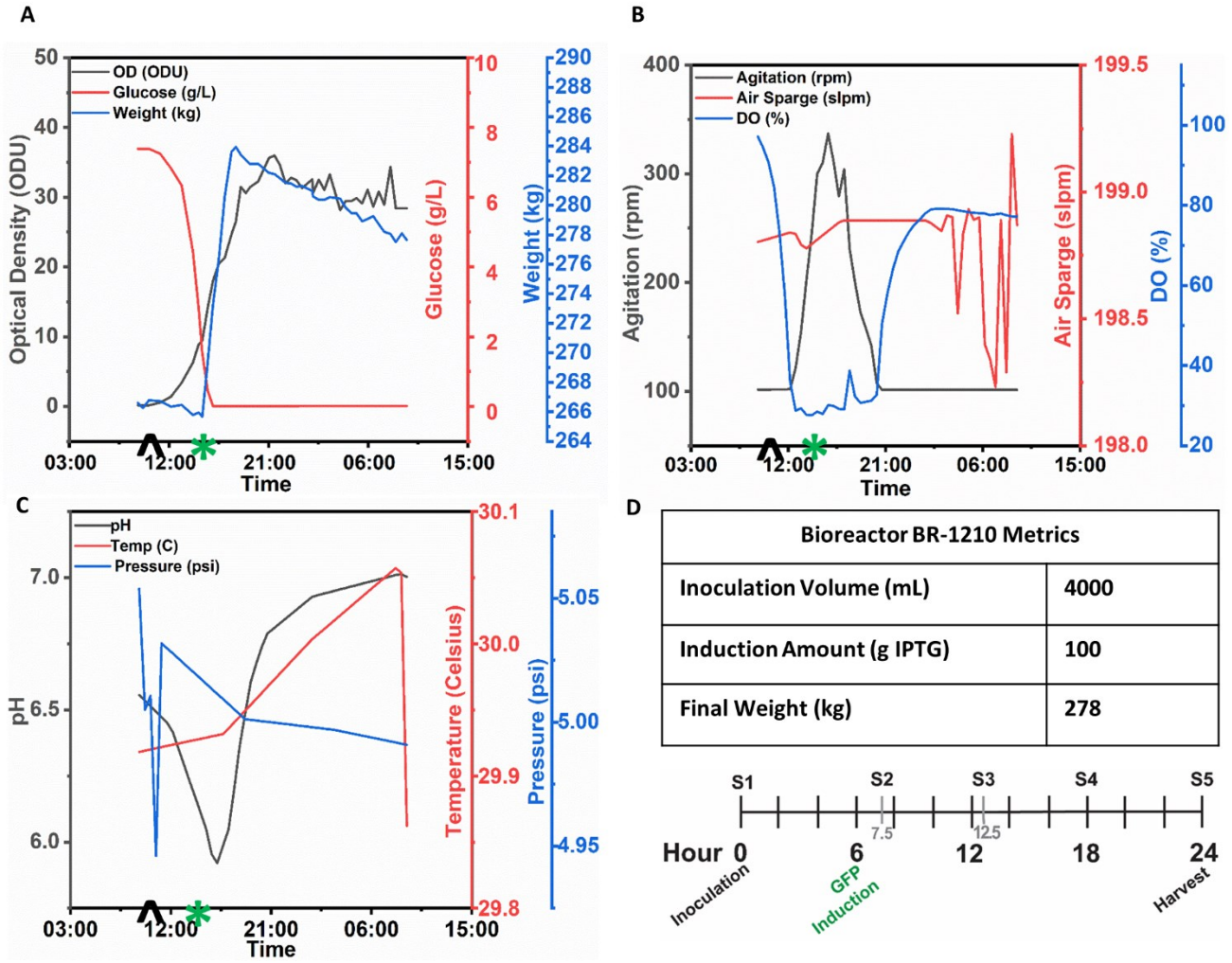

Bioreactor BR-1210 Metrics	
Inoculation Volume (mL)	4000
Induction Amount (g IPTG)	100
Final Weight (kg)	278

Figure 3. Parameters measured during the bioreactor run, highlighting changes during inoculation at 09:08 (^) and induction at 15:08 (*). *a) Optical density increased drastically after induction and levelled out afterwards, while glucose sharply declined after induction. Weight remained within 275 kg +/- 10 kg range. Fluctuations in weight are due to standard variability within measurement. b) Agitation, Air Sparge and Dissolved Oxygen were all monitored throughout the bioreactor run. The sharp decrease in DO% after inoculation levels out after induction which then increases after an increase in agitation. Air sparge remains at a steady rate and begins to vary towards the end of the process before final harvest. c) Changes in pH, temperature and pressure were all tightly monitored and maintained throughout the bioreactor run but do show a decline in pH and pressure after inoculation. Pressure begins to rise and level out immediately after inoculation while pH slowly declines until after induction and then begins to rise and level out until final harvest. The temperature remains within the strict 29.8 and 30.1 Celsius range. Table 4.D gives a brief overview of other important parameters measured for this run. The timeline in 4.D shows inoculation began at hour 0, GFP induction at hour 6, and final harvest at hour 24. Time points for the five samples analyzed included hour 0, hour 7.5, hour 12.5, hour 18 and hour 24.*

Results in Figure 3A show a correlation between glucose decline and an increase in optical density and weight (measured by settling of cells on the bottom of the bioreactor). This is expected, as glucose is consumed by cells during the proliferation period. Figure 3B depicts changes in dissolved oxygen (DO) as a percentage compared to agitation rpm which is inversely correlated. This relationship can be explained as when agitation and air sparging are introduced to the system, more dissolved air and therefore oxygen is added to the solution. These metrics are important to capture to ensure adequate functionality of the bioreactor and to give insight into the biological processes occurring during inoculation, GFP induction and thereafter.

Glucose levels correlate with cell proliferation because as cells are expanding, they are consuming glucose and therefore levels will decrease as cells proliferate. Optical Density (OD) also relates to *E. coli* proliferation as while cells are proliferating the optical density will increase due to a larger number of cells in the culture. Temperature monitoring is important for ensuring that the environment is suitable for cell proliferation. Other variables such as pressure, pH and DO % all must be tightly monitored and maintained within a certain range

for optimal *E. coli* health, protein expression and proliferation. As cells are expanding and consuming glucose and oxygen, the glucose and DO% levels will drop.

Plate Reader Assays

Results from the plate reader for bioreactor runs 1 and 2 are shown in Figure 4 and are considered offline analysis. OD and fluorescence intensity of *E.coli* suspended in the broth media were measured. Subsequently, the suspension was centrifuged to isolate the supernatant, which was then plated and measured separately. Technical triplicates were measured for each sample. The isolation and measurement of the supernatant fluorescence intensity is essential to infer potential GFP leakage from the *E.coli* into the broth media. It is well-established that bacterial membranes become more permeable as they undergo cellular death, leading to "leakage" in their surrounding media. [19], [20] Therefore, measuring fluorescence intensity in the supernatant can indicate the health of the cell population.

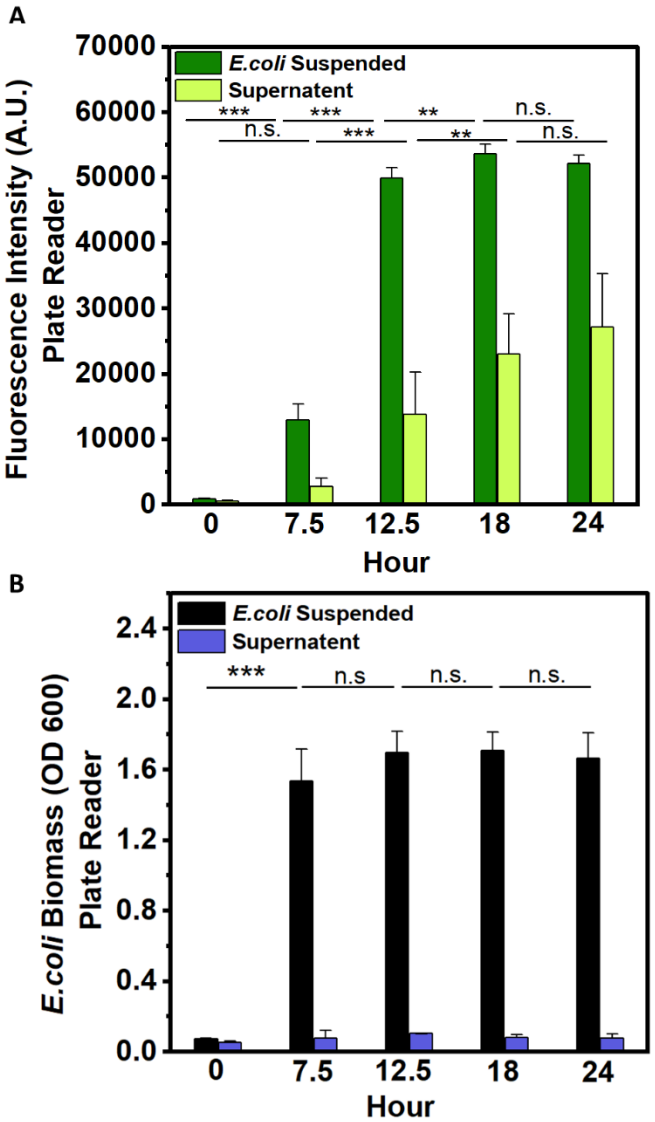

Figure 4. Bar graph representations of fluorescence intensity and OD for two different bioreactor runs collected via plate reader*. a). E. coli fluorescence values for 5 samples from bioreactor run 1 and 2 shows a significantly high (p<.001) relative fluorescence intensity of the suspended cell sample at hour 18 which is not significantly different than at hour 24 and a significant (p<.001) increase in fluorescence intensity of the supernatant at hour 18 which is not significantly greater than hour 24. b). E. coli OD values for 5 samples from bioreactor run 1 and 2 shows a significantly high (p<.0001) increase in OD value of the suspended cell sample at hour 7.5 which is not significantly different than hours 12.5, 18 or 24 indicating that cells proliferated and plateaued in growth after hour 7.5.*

The OD values of the cells suspended in broth, indicative of cell density, show comparable changes in density profiles for both bioreactor runs. There was no significant change in cell density values of the supernatant for both runs, indicating that the supernatant was successfully isolated. The OD values of the suspended cells indicate the samples taken at hours 12.5 and 18 had the highest ($p<.0001$) cell density for run 1 and hours 12.5, 18 and 24 had the highest ($p<.0001$) OD values for run 2 based on a repeated measures ANOVA and Tukey Means comparison. Run 1 shows no significant difference between OD values for hours 12.5 and 18 and run 2 shows no significant difference in OD values between 12.5, 18 and 24 hours. In run 1, there was a significant decline in cell density after hour 18 ($p<.0001$), suggesting potential cell death occurred. Fluorescence intensity values for bioreactor run 1 indicate a significantly higher ($p<.0001$) overall fluorescence at hour 18 for suspended cells and hour 24 for supernatant. While GFP expression in bioreactor run 2 peaks significantly at hour 12.5 for suspended cells and hour 24 for supernatant.

The OD and fluorescence intensity data obtained from the plate reader are part of the offline analysis of these bioreactor runs. The observed increase in fluorescence intensity of the supernatant across both bioreactor runs could indicate cell death or an increased membrane permeability, which is the highest at 24 hours (but not significantly higher than hour 18). The fluorescence intensity value of the suspended cells increases and peaks at hour 18 but thereafter does not significantly change at hour 24. These trends underscore the potential benefits of optimizing the duration of future bioreactor runs to enhance total product yield and streamline resource utilization in this bioprocess.

Statistical analysis, based on a Repeated Measures ANOVA with Tukey Means Comparison, was conducted on the technical triplicates from two separate biological runs collected for each time point via the plate reader. Comparison of each time point facilitated the identification of peak values for optical density (correlated with cell density) and fluorescence (associated with GFP expression).

Microscopy and Image Analysis Results

Image analysis was performed as a secondary method for quantification of relative fluorescence intensity, and cell density at each time point. Summary Figure 5 highlights this offline analysis pipeline from confocal image capture through image analysis for samples collected from both bioreactor runs. Raw images were first collected for every sample using both λ_{ex} = 488 nm; λ_{em} = 507 nm and λ_{ex} = 642 nm; λ_{em} = 662 nm which produced two separate images for each region. Individual cells were identified based the CellBrite 640 membrane stain. This membrane stain was used as a marker for the *E.coli*.

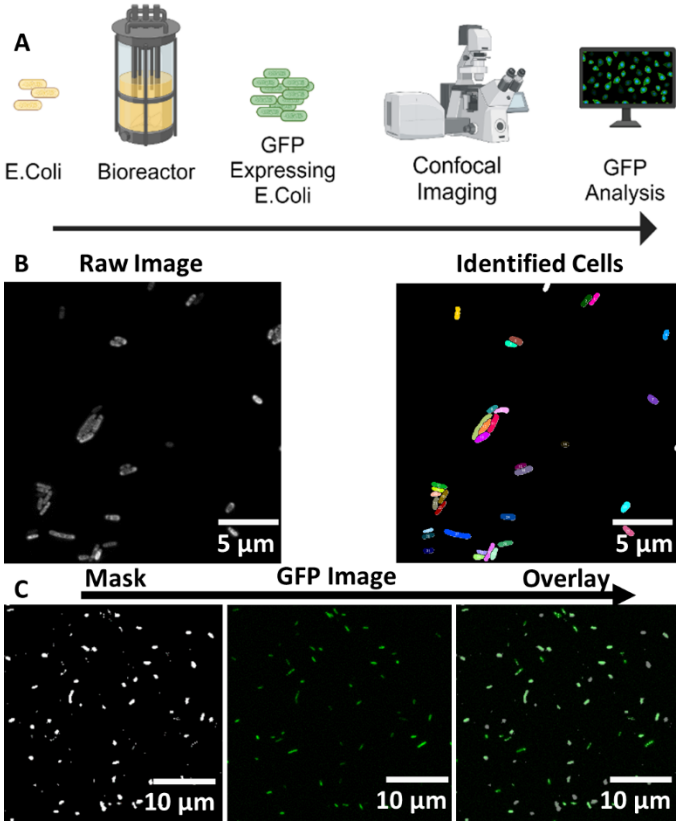

Figure 5. Offline image analytics process for calculating fluorescence intensity per cell and cell count*. a) Samples are collected from the bioreactor at various time points and analyzed using confocal microscopy. b) Raw images collected are processed using python code in Image J to identify each individual E. coli cell based on the CellBrite 640 membrane stain. c) The identified cells then are used as a "mask" which when overlayed with the EGFP fluorescence image will measure the relative mean fluorescence intensity per E. coli.*

Once individual cells were identified, these identified cells were made into a cell mask. This mask was then overlayed on top of the EGFP image of the same region. Each individual cell, marked with the mask and overlayed on the EGFP image was then measured for fluorescence intensity. The code described earlier allows for repeatable fluorescence intensity measurements for each individual image for all samples. This method for measuring fluorescence allows for a higher resolution offline analysis as compared to the plate reader fluorescence intensity data. The confocal image analysis of fluorescence intensity per cell can be used to measure the distribution of fluorescence per cell as opposed to the overall fluorescence intensity per well measured in the plate reader. Multiple images were collected for each sample to accumulate hundreds of cells for fluorescence intensity analysis.

Image analysis of fluorescence intensity for two separate bioreactor runs can be seen in Figure 6. Fluorescent intensity data from both bioreactor runs follow a similar trend. Specifically, the highest mean fluorescence intensity can be found at hour 12.5 (p<.0001). The statistical analysis was performed via repeated measure ANOVA and Tukey Means Comparison with an alpha of .05.

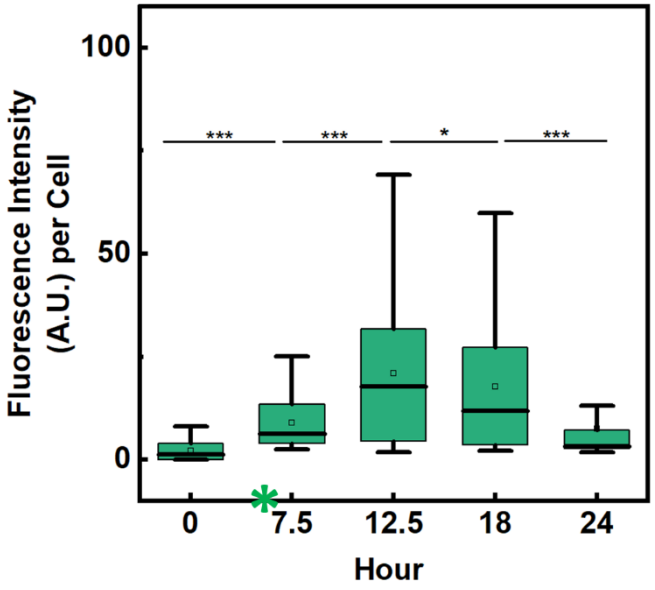

Figure 6. Fluorescence intensity per cell calculated using confocal image analysis for two separate bioreactor runs. *a) The peak of fluorescence intensity (A.U.) per E. coli for both runs is at hour 12.5 (p<.0001) which then begins to significantly decline at hour 18 (p<.05).*

Overall, the fluorescence intensity per cell area measured at five different time points (hour 0, 7.5, 12.5, 18, and 24) revealed significant variations (Repeated Measures ANOVA and Tukey Means Comparison, $p < 0.0001$) between all time points for the two runs. Fluorescence intensity data shows a distinct peak in fluorescence intensity at the 12.5-hour time point. After fluorescence reached its maximum levels at hour 12.5, the fluorescence intensity begins significantly declining in hours 18 and 24.

These results indicate that peak GFP expression per *E.coli* is around the 12.5 hour period post inoculation. This peak in fluorescence intensity per cell area is different than the peak in overall fluorescence measured with the plate reader, which showed a peak at hours 18 and 24. This difference can be attributed to the fact that the plate reader takes a singular reading of fluorescence intensity of an entire sample and is much lower resolution than the confocal fluorescence intensity measurement per cell area. Although the overall fluorescence intensity may increase during hours 18 and 24, this does not account for any cellular membrane leakage or levels of proliferation that could impact the final measurement.

To calculate cell density per sample, a standardized number of images were used. Initially, 56 individual images were captured, and the total cell number was calculated per image using the cell mask process previously described. This cell density quantification method provides a total cell count per image as opposed to an OD

value per well measured in the plate reader. This offline analysis method was used to both give higher resolution and a means of comparison for the data captured through plate reader analysis. Samples from hour 0 were diluted 10-fold less than all other samples due to lack of cell density and therefore cell counts per image were divided by 10.

After images were captured and analyzed, a sample of 50 images randomly selected were compiled to determine the distribution of cell count per image. Additionally, a sample of the remaining 6 images were compiled to determine the distribution of cell count per image. The results from these two sample sizes were compared. The results from the 50-image sample size were more normally distributed than the results from the 6-image sample size and show more significance in the difference between the groups as seen in Figure 7.

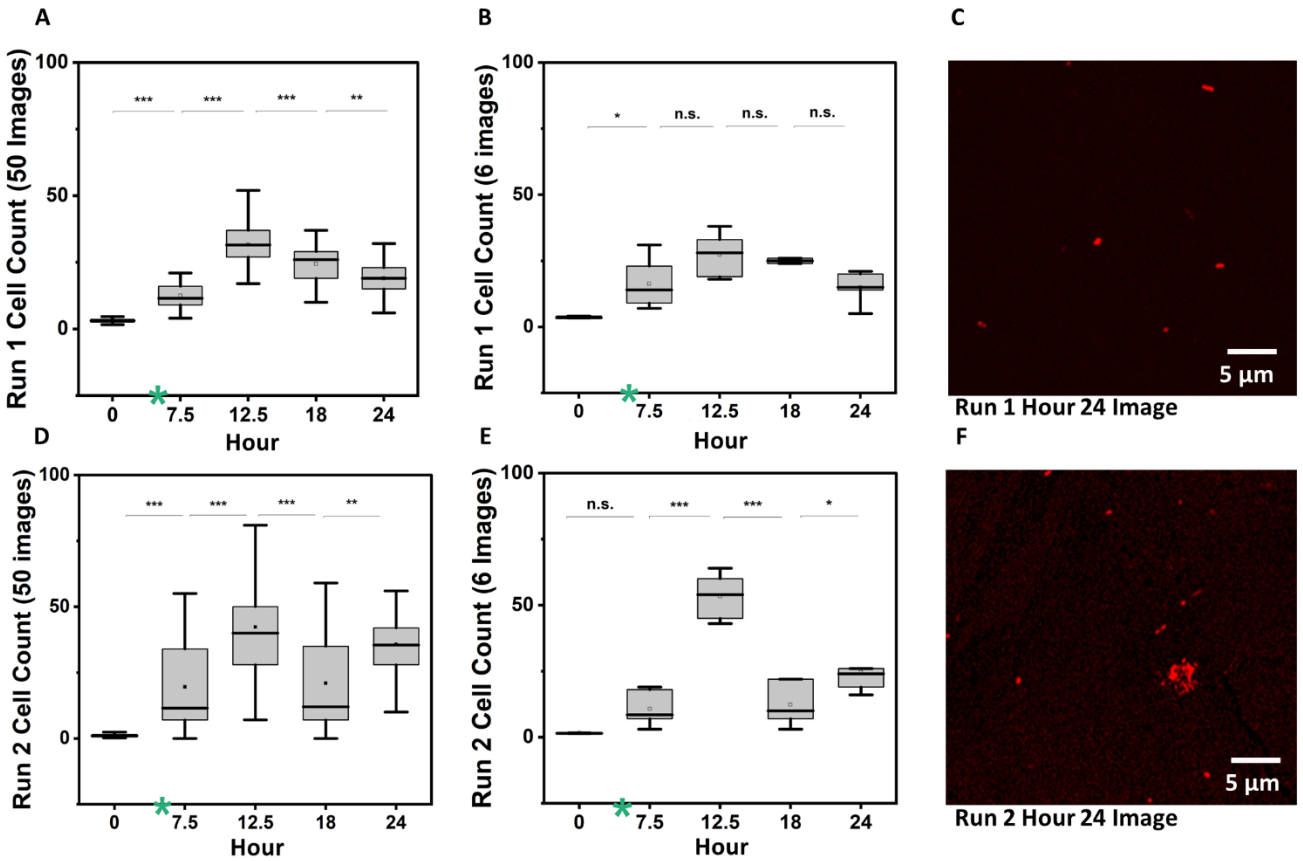

Figure 7. Cell count per image analyzed at different sample sizes for two bioreactor runs. *a) In run 1, with a 50-image sample size, the peak in cell number per image is observed at hour 12.5 (p<.0001). b) In run 1, based on a 6-image sample size, determination of the peak in cell number is inconclusive due to a non-significant difference in cell number when comparing hours 7.5, 12.5, 18, and 24. c) Hour 24 image of E.coli from run 1 showing intact E.coli which are fairly sparse. d) In run 2, also with a 50-image sample size, the peak in cell number per image is observed at hour 12.5 (p<.0001). e) Conversely, in run 2, based on a 6-image sample size, a peak is observed at hour 12.5 for cell number per image (p < .0001). f) Hour 24 image of E.coli from run 2 showing cells potentially beginning to die via apoptosis showing multiple cell fragments which can impact the cell mask and cell count.*

Results from the 50-image sample size show the highest cell count per image to be at hour 12.5 for both run 1 (Repeated Measures ANOVA and Tukey Means Comparison, p<.0001) and run 2 (p <.0001). Analysis of 6 image sample size for run 2 shows the highest cell count per image to be at hour 12.5 (p<.0001). However, when analyzing the 6-image sample size for run 1, there is no significant difference between hours 7.5, 12.5, 18 and 24. Therefore, in order to determine the highest cell count per image, more than 6 images are necessary. These results of cell count per image follow a similar trend to the OD data from the plate reader analysis which both correlate to cell density. This information further supports the claim that there may be a point of diminishing returns during this bioreactor where cell density begins to decrease due to increased cell death. Figure 7 highlights the cell fragments at hour 24 that begin to appear in run 2 and can impact the cell mask and subsequent count.

Comparison of Analytical Methods

For a comprehensive review of the bioreactor performance and *E.coli* response, both inline and offline results were compared. Figure 8 highlights run 2 metrics including optical density and fluorescence metrics from various measurement sources. In comparing these results there is a clear peak in both cell density and fluorescence intensity around hours 12.5 and 18. The multifaceted analysis and comparison of several metrics, gives a higher resolution view of this bioprocess, which can be used for further optimization and enhancement in the future. This short study combines two methods for fluorescence intensity quantification which correlates with GFP expression which could indicate optimal bioreactor settings with further investigation. This data suggests it might be optimal to shorten this bioprocessing timeline to improve GFP expression and *E.coli* viability, however more data collected from future runs will be necessary to validate this claim. The limitations of this study include sample size, which was constrained by only two biological runs.

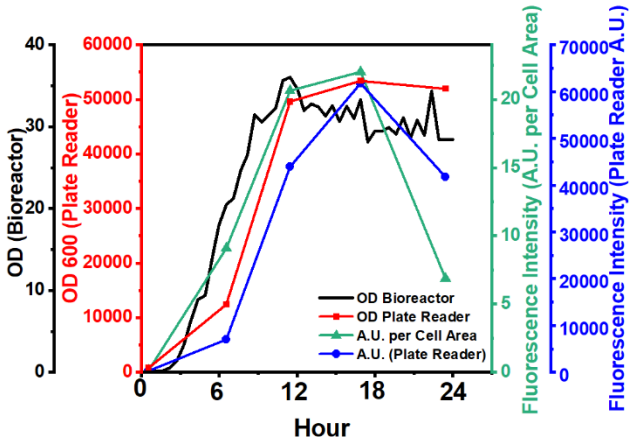

Figure 8. Results from bioreactor run 2 including both inline and offline data. *OD and fluorescence intensity data collected using a plate reader, OD data collected inline from the bioreactor, and fluorescence intensity per cell computed via confocal image analysis were all compared over time and show a peak in values between hours 12.5 and 18.*

4. CONCLUSION

Analysis of plate reader data, confocal image processing data and inline bioreactor data suggest that the peak *E. coli* density and GFP expression are between hours 12.5 and 18. There is a decline in both GFP expression and *E. coli* density after hour 18, suggesting that the 24-hour period may not be conducive to optimal protein expression or cell viability. As the cells are proliferating, there may be a point where they become overpopulated or underfed and start not only decreasing their rate of proliferation but also begin to die. This idea can be supported by the supernatant fluorescence intensity data, which shows a steady increase in GFP expression over time. This increased supernatant fluorescence intensity could indicate the *E. coli* have increased membrane permeability and are therefore “leaking” into the surrounding media or are dying from apoptosis and internal protein is integrating with the media. [19, 20] Future iterations of this bioreactor run should take this information into account to optimize the bioreactor parameters and timeframe from inoculation to harvest. This study was restricted to only two bioreactor runs as this bioprocess is only intermittently scheduled. Therefore, analyzing biological triplicates was not possible and drove the team to analyzing biological duplicates and sampling triplicates. Future implications of this study could look at biological triplicate analysis to confirm these results.

5. ACKNOWLEDGEMENTS

G.R was supported by the Chemistry of Life Pre-Doctoral Training Grant at NC State University (NIH Grant 5T32GM141887-03). This work was performed in part at the North Carolina State University BTEC Facility. The authors wish to acknowledge the support provided by the Novo Nordisk Foundation (Grant NNF19SA0035474) and National Science Foundation (Grant EBMS- 2033997).

6. REFERENCES

[1] I. Ganeeva, E. Zmievskaya, A. Valiullina, A. Kudriaeva, R. Miftakhova, A. Rybalov, E. Bulatov, Recent Advances in the Development of Bioreactors for Manufacturing of Adoptive Cell Immunotherapies, Bioengineering 9(12) (2022) 808.

[2] A. Aijaz, M. Li, D. Smith, D. Khong, C. Leblon, O.S. Fenton, R.M. Olabisi, S. Libutti, J. Tischfield, M.V. Maus, R. Deans, R.N. Barcia, D.G. Anderson, J. Ritz, R. Preti, B. Parekkadan, Biomanufacturing for clinically advanced cell therapies, Nature Biomedical Engineering 2(6) (2018) 362-376.

[3] S. Mitra, G.S. Murthy, Bioreactor control systems in the biopharmaceutical industry: a critical perspective, Systems Microbiology and Biomanufacturing 2(1) (2022) 91-112.

[4] I. Clegg, Process analytical technology, Specification of Drug Substances and Products2020, pp. 149-173.

[5] Y.-R. Li, Z.S. Dunn, Y. Zhou, D. Lee, L. Yang, Development of Stem Cell-Derived Immune Cells for Off-the-Shelf Cancer Immunotherapies, Cells 10(12) (2021) 3497.

[6] D.L. Wagner, U. Koehl, M. Chmielewski, C. Scheid, R. Stripecke, Review: Sustainable Clinical Development of CAR-T Cells – Switching From Viral Transduction Towards CRISPR-Cas Gene Editing, Frontiers in Immunology 13 (2022).

[7] J. Xu, X. Xu, C. Huang, J. Angelo, C.L. Oliveira, M. Xu, X. Xu, D. Temel, J. Ding, S. Ghose, M.C. Borys, Z.J. Li, Biomanufacturing evolution from conventional to intensified processes for productivity improvement: a case study, mAbs 12(1) (2020) 1770669.

[8] O. Khanal, A.M. Lenhoff, Developments and opportunities in continuous biopharmaceutical manufacturing, MAbs 13(1) (2021) 1903664.

[9] G. Gerzon, Y. Sheng, M. Kirkitadze, Process Analytical Technologies - Advances in bioprocess integration and future perspectives, J Pharm Biomed Anal 207 (2022) 114379.

[10] P. Biechele, C. Busse, D. Solle, T. Scheper, K. Reardon, Sensor systems for bioprocess monitoring, Engineering in Life Sciences 15(5) (2015) 469-488.

[11] E.J. Kim, J.H. Kim, M.-S. Kim, S.H. Jeong, D.H. Choi, Process Analytical Technology Tools for Monitoring Pharmaceutical Unit Operations: A Control Strategy for Continuous Process Verification, Pharmaceutics 13(6) (2021) 919.

[12] S. Hisiger, M. Jolicoeur, A multiwavelength fluorescence probe: is one probe capable for on-line monitoring of recombinant protein production and biomass activity?, J Biotechnol 117(4) (2005) 325-36.

[13] T. Broger, R.P. Odermatt, P. Huber, B. Sonnleitner, Real-time on-line flow cytometry for bioprocess monitoring, J Biotechnol 154(4) (2011) 240-7.

[14] H. Reischer, I. Schotola, G. Striedner, F. Potschacher, K. Bayer, Evaluation of the GFP signal and its aptitude for novel on-line monitoring strategies of recombinant fermentation processes, J Biotechnol 108(2) (2004) 115-25.

[15] B.J. Feilmeier, G. Iseminger, D. Schroeder, H. Webber, G.J. Phillips, Green Fluorescent Protein Functions as a Reporter for Protein Localization in *Escherichia coli*, Journal of Bacteriology 182(14) (2000) 4068-4076.

[16] G. Faust, A. Stand, D. Weuster-Botz, IPTG can replace lactose in auto-induction media to enhance protein expression in batch-cultured *Escherichia coli*, Engineering in Life Sciences 15(8) (2015) 824-829.

[17] G.N.L. Rosano, E.A. Ceccarelli, Recombinant protein expression in Escherichia coli: advances and challenges, Frontiers in Microbiology 5 (2014).

[18] O.A. Savchuk, O.F. Silvestre, R.M.R. Adão, J.B. Nieder, GFP fluorescence peak fraction analysis based nanothermometer for the assessment of exothermal mitochondria activity in live cells, Scientific Reports 9(1) (2019).

[19] J.S. Webb, S.R. Barratt, H. Sabev, M. Nixon, I.M. Eastwood, M. Greenhalgh, P.S. Handley, G.D. Robson, Green Fluorescent Protein as a Novel Indicator of Antimicrobial Susceptibility in *Aureobasidium pullulans*, Applied and Environmental Microbiology 67(12) (2001) 5614-5620.

[20] M. Lowder, A. Unge, N. Maraha, J.K. Jansson, J. Swiggett, J.D. Oliver, Effect of Starvation and the Viable-but-Nonculturable State on Green Fluorescent Protein (GFP) Fluorescence in GFP-Tagged *Pseudomonas fluorescens* A506, Applied and Environmental Microbiology 66(8) (2000) 3160-3165.